

On the Achievable Rate of Multi-Antenna Receivers with Oversampled 1-Bit Quantization

Sandra Bender, Meik Dörpinghaus, and Gerhard Fettweis

Vodafone Chair Mobile Communications Systems, SFB 912 HAEC, Technische Universität Dresden, Germany

Email: {sandra.bender, meik.doerpinghaus, gerhard.fettweis}@tu-dresden.de

Abstract—We analyze the spectral efficiency of a 1-bit quantized multiple-input multiple-output channel with oversampling in time, where 1-bit quantization could become a key component to achieve the energy efficiency that is required for future communication systems. Applying adapted signaling schemes and appropriate power allocation algorithms, we derive lower bounds on the spectral efficiency based on results for the single-input single-output case. We show the potential gain compared to previous results without oversampling.

Index Terms—A/D-conversion, oversampling, runlength-coding, MIMO

I. INTRODUCTION

Communication in the mmWave range at 60 GHz continues to draw attention, especially in combination with multiple-input multiple-output (MIMO) systems, for achieving data rates in the order of tens of Gbit/s; hence, its relevance in the standardization process, e.g., for the fifth generation mobile standard (5G) or for the IEEE 802.11ay, where the latter is planned to be released this year [1]. One advantage of the 60 GHz band is the amount of unlicensed spectrum available, which holds even more if taking this one step further to the range of 100-300 GHz carrier frequency, which is promising for applications like wireless communications between computer boards within a server [2].

However, when it comes to the likewise important topic of energy efficiency, the increased bandwidth results in a bottleneck in terms of energy consumption at the analog-to-digital converter (ADC). The consumed energy per conversion step increases with sampling frequency and converter resolution [3]. The effect scales with the MIMO-scenario, as one ADC is required for every data stream. This and the small voltage headroom of downscaled CMOS technology [4] make signaling schemes adapted to 1-bit quantizers an attractive alternative. We are mainly interested in the achievable rate of such a coarsely quantized system, which is analyzed in terms of capacity bounds in [5] and [6] analytically and in [7]–[9] by simulations for different scenarios, where [9] considers spatial oversampling.

For the case of single-input single-output systems, oversampling in time domain of a 1-bit quantized receive signal has been shown to increase the achievable rate for the noiseless case already in [10] and [11]. It has been further studied in [12] for the low SNR domain analytically and in [13], [14] by simulation, where gains in terms of achievable rate w.r.t. Nyquist sampling were observed. Despite this, to the best of our knowledge, there are no analytic capacity bounds for temporally oversampled MIMO channels available. In

this work, we thus evaluate the performance by deriving lower bounds on the achievable rate for signaling schemes applying oversampling w.r.t. Nyquist-sampling in the context of 1-bit quantized MIMO schemes. These signaling schemes are not necessarily capacity-achieving. Our contribution can be summarized as follows:

- Extension of the spectral efficiency results for 1-bit quantized SISO channels with oversampling in time to the MIMO scenario.
- Analysis of the performance of different channel equalization and power allocation schemes.
- Optimization of the power allocation for the case that no channel equalization can be carried out at the receiver.

We apply the following notations: vectors and matrices are set bold, random variables sans serif. \mathbf{X}^K is a random vector of length K . For information measures, $(\cdot)'$ denotes the corresponding rate. Further, $(\cdot)^H$ denotes the Hermitian transpose of a matrix and $\text{diag}(\mathbf{x})$ is a diagonal matrix with the vector \mathbf{x} specifying the main diagonal.

II. SYSTEM MODEL

We consider a bandlimited complex $N_r \times N_t$ MIMO channel with 1-bit quantization and oversampling at the receiver, where N_r and N_t are the numbers of receive and transmit antennas, respectively. The system model is depicted in Fig. 1. All components, i.e., mapper, ADC, and demapper, process the in-phase and quadrature components of the signal separately. For both, in-phase and quadrature component, 1-bit quantization only allows to resolve the sign of the signal. The transmitted information is effectively encoded in the position of the zero-crossings (ZC) of the real and imaginary part of the transmitted signal. We therefore consider as input signal sequences, which contain the distances of consecutive ZCs. The resolution T_{res} with which these distances can be specified, depends on the oversampling factor M of the system, which is defined w.r.t. the one-sided signal bandwidth W of the lowpass (LP) filters at the transmitter and receiver

$$T_{\text{res}} = \frac{1}{M f_{\text{Nyq}}} = \frac{1}{2WM} \quad (1)$$

where $f_{\text{Nyq}} = 2W$ is the Nyquist rate corresponding to the receive filter bandwidth. The extreme cases hereby are $M \rightarrow \infty$, i.e., $T_{\text{res}} \rightarrow 0$, representing infinite oversampling and, hence, a continuous-time channel, and $M = 1$, representing Nyquist-sampling. For every input, two input sequences $\mathbf{A}_{i,\mathcal{R}}^K$ and $\mathbf{A}_{i,\mathcal{I}}^K$ are mapped onto a complex signal $x_i(t)$, that is suited for

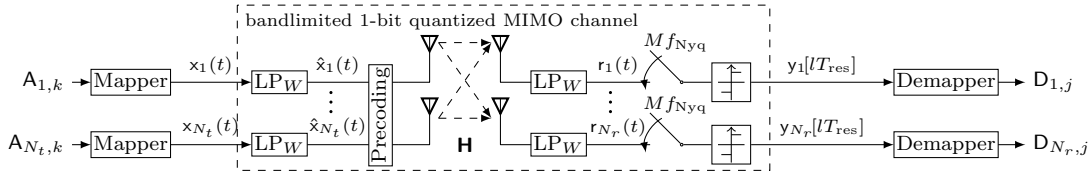


Fig. 1. System model

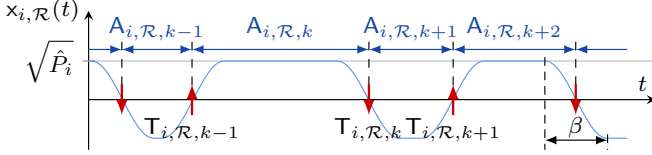


Fig. 2. Mapping from input sequence $\mathbf{A}_{i,\mathcal{R}}^{(K)}$ to $x_{i,\mathcal{R}}(t)$

transmission over the channel. For real and imaginary part of $x_i(t)$, the transitions between two levels $\pm\sqrt{\hat{P}_i}$ exactly correspond to the ZC-distances specified in $\mathbf{A}_{i,\mathcal{R}}^K$ and $\mathbf{A}_{i,\mathcal{I}}^K$, i.e.,

$$x_{i,\mathcal{R}/\mathcal{I}}(t) = \left(\sum_{k=1}^K \sqrt{\hat{P}_i} (-1)^k g(t - \mathsf{T}_{i,\mathcal{R}/\mathcal{I},k}) \right) + \sqrt{\hat{P}_i} \quad (2)$$

where $g(\cdot)$ is the transition waveform and $\mathsf{T}_{i,\mathcal{R}/\mathcal{I},k} = \sum_{w=1}^k \mathbf{A}_{i,\mathcal{R}/\mathcal{I},w}$ the time instant of the k th ZC. One possible mapping of the real signal component is depicted in Fig. 2. The average transmit power of $x_i(t)$ depends on the transition waveform and the ratio between transition β time and hold time of the level $\pm\sqrt{\hat{P}_i}$. In the remainder of this work, we will focus on two special cases

1) *Continuous Time Channel*: It represents a limiting case in the sense of infinite oversampling ($M \rightarrow \infty$) as then the maximum temporal resolution is available at the receiver. We consider exponential distributed ZC-distances $\mathbf{A}_{i,k}$, which maximizes the input entropy, with parameter λ , s.t. $\mathbb{E}[\mathbf{A}_{i,k}] = 1/\lambda + \beta$ and a sine-based transition waveform [15]. As $T_{\text{res}} \rightarrow 0$, the transition time between the levels $\pm\sqrt{\hat{P}_i}$ is $\beta \gg T_{\text{res}}$, cf. Fig. 2. The filter bandwidth W is set to $1/2\beta$ allowing for neglecting of deletion errors, see Section III-A.

2) *Discrete Time Channel*: It represents a simple discrete-time and, thus, implementable scheme, where we sample such that the transition time $\beta = T_{\text{res}}$. We consider a runlength-limited input sequence with geometric distributed ZC-distances $\mathbf{A}_{i,k}$, which again corresponds to input entropy maximization. $\mathbb{E}[\mathbf{A}_{i,k}]$ then depends on the minimum runlength. The filter bandwidth W is set to the 90% power containment bandwidth of $x_i(t)$ given a triangular transition waveform [16].

The chosen input distribution determines the average symbol duration $T_{\text{avg}} = \mathbb{E}[\mathbf{A}_{i,k}]$. For the aforementioned scenarios the average transmit power of $x_i(t)$ per channel is given by

$$P_i = \begin{cases} 2 \frac{\frac{1}{2} + 2W\lambda^{-1}}{1 + 2W\lambda^{-1}} \hat{P}_i, & \text{(Scenario II-1)} \\ 2 \left(1 - \frac{2}{3\mathbb{E}[\mathbf{A}_{k,i}]} \right) \hat{P}_i, & \text{(Scenario II-2)} \end{cases} \quad (3)$$

After mapping, the signal $x_i(t)$ is LP-filtered by an ideal LP with one-sided bandwidth W in order to ensure bandlimitation. The filter output $\hat{x}_i(t)$ is transmitted via an $N_r \times N_t$ MIMO

channel with precoding. The sampled and quantized received signal $\mathbf{y} = [y_1[lT_{\text{res}}], y_2[lT_{\text{res}}], \dots, y_{N_r}[lT_{\text{res}}]]^T$ is given by

$$\mathbf{y} = Q_1(\mathbf{H}\mathbf{C}\hat{\mathbf{x}} + \hat{\mathbf{n}}) \quad (4)$$

where \mathbf{H} is the time-variant $N_r \times N_t$ channel matrix containing the complex Gaussian distributed channel coefficients at time lT_{res} , $\hat{\mathbf{x}} = [\hat{x}_1[lT_{\text{res}}], \hat{x}_2[lT_{\text{res}}], \dots, \hat{x}_{N_t}[lT_{\text{res}}]]^T$ and $\hat{\mathbf{n}}$ is the filtered and sampled zero-mean complex additive Gaussian noise vector with variance per sample $\sigma_{\hat{\mathbf{n}}}^2$. Due to bandlimitation and oversampling it is temporally correlated. $Q_1(\cdot)$ denotes a binary quantizer with threshold zero, i.e., $Q_1(x) = 1$ if $x \geq 0$ and $Q_1(x) = -1$ if $x < 0$, and \mathbf{C} denotes the precoding operation. For notional convenience, we omit the sampling time index l at \mathbf{H} , $\hat{\mathbf{x}}$, $\hat{\mathbf{n}}$ and \mathbf{y} . We assume full channel state information (CSI) at transmitter and receiver, as we are interested in short-range, quasi static and likely indoor communication scenarios as, e.g., in [2]. Channel estimation with 1-bit ADCs is a topic under active research, e.g., [17]–[20]. For very short range communication with line-of-sight component it has further been measured, that such channels can be considered largely frequency flat, despite the large bandwidth [21].

For every receive signal y_m , the positions of the ZCs of the real and imaginary component are mapped back onto vectors of distances $\mathbf{D}_{m,\mathcal{R}}$ and $\mathbf{D}_{m,\mathcal{I}}$. Note that possibly $K \neq J$, since the noise may add or remove ZCs. Neither of the above mentioned transmit signal waveforms $x_i(t)$ is hard bandlimited, hence, the LP-filter at the transmitter introduces a distortion to the signal due to the out-of-band energy filtered out. We capture this distortion by the mean squared error $\sigma_{\tilde{x}_i}^2$ of the signal $\tilde{x}_i(t) = x_i(t) - \hat{x}_i(t)$ and treat it as additional noise source, where

$$\sigma_{\tilde{x}_i}^2 = \frac{1}{\pi} \int_{2\pi W}^{\infty} S_{x_i}(\omega) d\omega \quad (5)$$

with $S_{x_i}(\omega)$ being the power spectral density of $x_i(t)$. Despite $\tilde{x}_i(t)$ not being independent of $x_i(t)$, by not exploiting this correlation we obtain a lower bound on the achievable rate. We assume the noise to be independent and identically distributed for all receive antennas, such that the signal-to-noise ratio (SNR) is defined as sum SNR w.r.t. the sum transmit power¹

$$\rho = \frac{P}{\sigma_{\hat{\mathbf{n}}}^2} \quad (6)$$

where $P = \mathbb{E}[|\mathbf{C}\hat{\mathbf{x}}|^2]$.

¹Note, that this definition is w.r.t. $x_i(t)$ and not $\hat{x}_i(t)$ as the LP-filter are treated as part of the channel and, thus, as additional noise source.

III. ACHIEVABLE RATE ON THE OVERSAMPLED MIMO-CHANNEL

The channel capacity is defined as the supremum of the mutual information rate over the joint distribution of all $\hat{x}_i(t)$, $i = 1 \dots N_T$, fulfilling the constraints of average power P and bandwidth W . The mutual information rate is defined as

$$I'(\mathbf{A}; \mathbf{D}) = \lim_{K \rightarrow \infty} \frac{1}{KT_{\text{avg}}} I(\mathbf{A}^K; \mathbf{D}^J) \quad (7)$$

with $I(\mathbf{A}^K; \mathbf{D}^J)$ being the mutual information. Furthermore, $\mathbf{A}^K = [\mathbf{A}_{1,\mathcal{R}}^K, \mathbf{A}_{1,\mathcal{I}}^K, \dots, \mathbf{A}_{N_t,\mathcal{R}}^K, \mathbf{A}_{N_t,\mathcal{I}}^K]$ and $\mathbf{D}^J = [\mathbf{D}_{1,\mathcal{R}}^J, \mathbf{D}_{1,\mathcal{I}}^J, \dots, \mathbf{D}_{N_r,\mathcal{R}}^J, \mathbf{D}_{N_r,\mathcal{I}}^J]$. As we consider two special cases with a given input distribution, we compute the achievable rate for each, which can be regarded as a lower bound on the capacity of the corresponding channels.

A. Achievable Rate for the SISO Channel

This section recalls results from [15], [16], [22] in order to prepare their application to the MIMO-channel. As the information symbols $A_{i,k}$ are the distances of the ZCs, we have to deal with three types of errors to evaluate (7):

- ZC-shifts, i.e., magnitude errors of the received symbol
- additional ZCs, leading to insertion of symbols
- extinction of a ZC pair, leading to deletion of symbols.

The capacity of insertion and deletion channels is still unknown, therefore we use the concept of the genie-aided receiver to lower-bound the achievable rate as in [23]. We provide the auxiliary information \mathbf{V} to the receiver, such that it can recognize the inserted or deleted symbols. Applying the chain rule, we can write for the mutual information rate in (7)

$$\begin{aligned} I'(\mathbf{A}; \mathbf{D}) &= I'(\mathbf{A}; \mathbf{D}, \mathbf{V}) - I'(\mathbf{A}; \mathbf{V} | \mathbf{D}) \\ &= I'(\mathbf{A}; \mathbf{D}, \mathbf{V}) - H'(\mathbf{V} | \mathbf{D}) + H'(\mathbf{V} | \mathbf{D}, \mathbf{A}) \quad (8) \\ &\geq I'(\mathbf{A}; \mathbf{D}, \mathbf{V}) - H'(\mathbf{V}) \quad (9) \end{aligned}$$

where (9) holds since conditioning cannot increase entropy and due to the non-negativity of entropy in case the auxiliary process \mathbf{V} can be modeled as a discrete valued process. This is the case in both scenarios as we will discuss subsequently.

1) *Achievable Rate of the Continuous-Time Model:* This scenario focuses on the mid to high SNR domain. We omit deletions, as they occur with negligible probability due to the bandlimited channel [22]. Then, $I'(\mathbf{A}; \mathbf{D}, \mathbf{V})$ captures the impact of approximately Gaussian distributed magnitude errors of the ZC-distances contained in \mathbf{D} on the mutual information. $H'(\mathbf{V})$ is the entropy rate of a process capturing the number of inserted symbols per transmit symbol $A_{i,k}$. In [15] we obtain a lower bound on $I'(\mathbf{A}; \mathbf{D}, \mathbf{V})$ and an upper bound on $H'(\mathbf{V})$. In the following we choose $W/\lambda = 0.7$ as we found that this maximizes the spectral efficiency for this setup [22].

2) *Achievable Rate of the Discrete-Time Model:* Here, we consider runlength encoded binary symbols, cf. [24]. Despite the correlation of the noise samples, we treat them as independent to obtain a lower bound on the achievable rate. With side information for every sample, we can reconstruct \mathbf{A} by knowing \mathbf{D} and \mathbf{V} s.t. $I'(\mathbf{A}; \mathbf{D}, \mathbf{V}) = H'(\mathbf{A})$. With (9), it

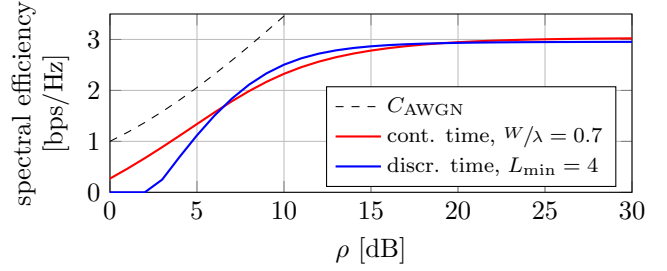


Fig. 3. Lower bounds on the spectral efficiency of the AWGN SISO channel for the continuous-time and discrete-time model

results $I'(\mathbf{A}, \mathbf{D}) \geq H'(\mathbf{A}) - H'(\mathbf{V})$. Most simply, \mathbf{V} can be a binary sequence, indicating which samples are flipped and which not. We choose $L_{\min} = 4$ as this maximizes the spectral efficiency, resulting in an oversampling factor $M = 3.21$ [16].

In order to compare both scenarios, we consider a lower bound on the spectral efficiency

$$SE = \frac{I'(\mathbf{A}; \mathbf{D})}{2W}. \quad (10)$$

The resulting lower bounds on the spectral efficiency are depicted in Fig. 3. They exceed the conventional 2 bit for the 1-bit quantized complex AWGN channel without oversampling. Furthermore, the lower bound for the discrete-time case exceeds the one for the continuous-time case in the mid SNR range, which can be either due to the lower-bounding or the reduced sampling resolution could actually reduce the noise sensitivity for the given input scheme in a certain SNR range.

B. MIMO Channel Decomposition

The capacity of the MIMO channel without output quantization is known to be achieved by circular-symmetric complex Gaussian input symbols with covariance matrix $\mathbf{R}_x = \mathbf{W}\mathbf{P}\mathbf{W}^H$, where \mathbf{W} is given by the singular value decomposition (SVD) of $\mathbf{H} = \mathbf{U}\mathbf{\Sigma}\mathbf{W}^H$. Here, \mathbf{U} and \mathbf{W} are unitary and the diagonal matrix $\mathbf{\Sigma}$ contains the individual channel weights σ_v , which are the singular values of \mathbf{H} . The transmit and receive signals can be pre- and post-processes such, that $\nu = \text{rank}(\mathbf{H}) \leq \min(N_t, N_r)$ independent, non-interfering channels result. The receive SNR on the channel v is given by $\rho_{v,\text{rx}} = \sigma_v^2 \frac{P_v}{\sigma_n^2}$. The remaining question is then to find an appropriate power distribution $\mathbf{P} = \text{diag}(P_1, \dots, P_\nu)$ among those channels.

With 1-bit quantization, however, the post-processing in form of multiplication with \mathbf{U}^H cannot be carried out on the quantized signal, which is why we consider it mainly for theoretical comparison. It is thus not depicted in Fig. 1. Instead, channel equalization can be carried out at the transmitter by channel inversion (CI) at the cost of potentially increased transmit power or a lesser receive SNR, respectively, as the different channel weights σ_v cannot be leveraged and $\rho_{v,\text{rx}} = \frac{P_v}{\sigma_n^2}$. In both cases, the achievable rate is given by the sum rate of the achievable rates on the individual channels

$$I'(\mathbf{A}; \mathbf{D}) = \sum_{v=1}^{\nu} I'(\mathbf{A}_v; \mathbf{D}_v). \quad (11)$$

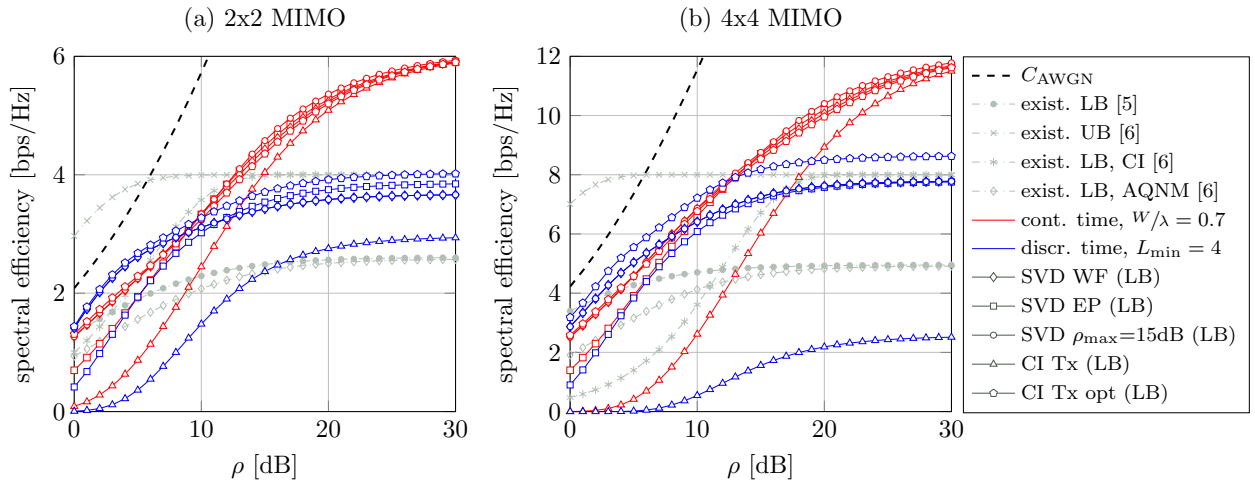


Fig. 4. Lower bounds on the spectral efficiency of the (a) 2x2 and (b) 4x4 MIMO channel for discrete and continuous-time scenarios, compared to an existing upper bound (UB) [6] and lower bounds (LB) based on Busgang decomposition [5], CI and an Additive Quantization Noise Model (AQNM) [6]

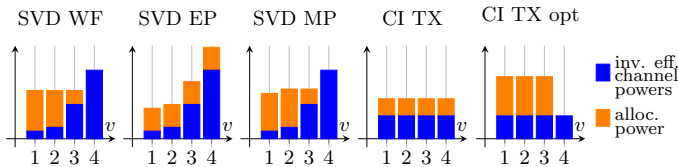


Fig. 5. Schematic illustration of the applied power allocation schemes

Eq. (11) is evaluated in terms of lower bounds, cf. (9), for different power allocation schemes in Section IV.

C. Power Allocation Schemes

Waterfilling is known to be optimal for the AWGN channel without quantization and Gaussian distributed input symbols. However, due to 1-bit quantization all amplitude information is discarded at the receiver such that waterfilling is not necessarily optimal anymore. We therefore analyze the performance of the following power allocation schemes with illustrations given in Fig. 5:

- 1) SVD with waterfilling (SVD WF)
- 2) SVD with equal power allocation (SVD EP)
- 3) SVD with a maximum effective channel SNR (SVD ρ_{\max}), where no more power is assigned to a channel if it has a maximum receive SNR $\rho_{v,rx} = \rho_{\max}$ as long as not every channel has this maximum receive SNR
- 4) CI at the transmitter distributing the power equally between all ν channels (CI Tx)
- 5) CI at the transmitter using only a subset of the ν channels such that the sum rate is maximized (CI Tx opt).

IV. NUMERICAL RESULTS

Lower bounds on the performance of the 1-bit quantized, temporally oversampled MIMO channel are evaluated based on the signaling schemes presented in Section III and applying the aforementioned power allocation schemes. The results for a 2x2 and 4x4 MIMO channel are depicted in Fig. 4. In contrast to an unquantized system, we observe that under 1-bit quantization, waterfilling is not generally the optimal scheme for power allocation. Due to the very limited

amplitude resolution of 1-bit, the achievable rate and, thus, the spectral efficiency per individual channel, saturate quickly over the SNR. Thus, it can be more efficient to either allocate the available transmit power equally to all channels or to define a maximum receive SNR and allocate the transmit power to other channels if it is exceeded. With regard to transmitter CI, using a subset of the ν available channels turns out to compensate for the expected loss of performance due to the reduced effective SNR. In the discrete scenario, it even outperforms all other power allocation schemes. The obtained lower bounds, except for CI Tx, outperform in some or all SNR regimes the lower bounds and partly even an upper bound on the spectral efficiency of 1-bit quantized MIMO channels without oversampling known from literature. This shows that 1-bit quantization in combination with oversampling is an appropriate scheme for energy-efficient high speed communication and that it can be applied to MIMO channels, even with the reduced signal processing capabilities at the receiver.

V. CONCLUSION

In the present work, we have studied the spectral efficiency of MIMO channels with 1-bit quantization and oversampling in time by extending our previous results on the achievable rate of the oversampled 1-bit quantized SISO channel. We show its applicability to MIMO, even without performing channel equalization operations at the receiver by using appropriate power allocation schemes. The derived lower bounds on the spectral efficiency partly outperform bounds known for Nyquist sampling. This underlines the potential of oversampling in time for compensating the inherent rate reduction of 1-bit quantization while increasing the energy efficiency compared to high resolution ADCs.

ACKNOWLEDGMENT

This work has been supported by the German Research Foundation (DFG) in the Collaborative Research Center "Highly Adaptive Energy-Efficient Computing", SFB912, HAEC.

REFERENCES

- [1] IEEE P802.11 - Task Group ay, "Status of project IEEE 802.11ay," Jun. 2017. [Online]. Available: http://www.ieee802.org/11/Reports/tgay_update.htm
- [2] M. Jennings, B. Klein, R. Hahnel, D. Plettemeier, D. Fritsche, G. Tretter, C. Carta, F. Ellinger, T. Nardmann, M. Schroter, K. Nieweglowski, K. Bock, J. Israel, A. Fischer, N. U. Hassan, L. Landau, M. Dörpinghaus, and G. Fettweis, "Energy-efficient transceivers for ultra-high-speed computer board-to-board communication," in *Proc. of the IEEE Int. Conf. on Ubiquitous Wireless Broadband (ICUWB)*, Montreal, Canada, Oct. 2015.
- [3] B. Murmann, "ADC performance survey 1997-2016," 2016. [Online]. Available: <http://web.stanford.edu/~murmman/adcsurvey.html>
- [4] R. Staszewski, "Digitally intensive wireless transceivers," *IEEE Design & Test of Computers*, vol. 29, no. 6, pp. 7–18, Dec. 2012.
- [5] A. Mezghani and J. A. Nossek, "Capacity lower bound of MIMO channels with output quantization and correlated noise," in *Proc. IEEE Int. Symp. Inform. Theory (ISIT)*, Boston, USA, Jul. 2012.
- [6] J. Mo and R. W. Heath, "Capacity analysis of one-bit quantized MIMO systems with transmitter channel state information," *IEEE Trans. on Signal Process.*, vol. 63, no. 20, pp. 5498–5512, 2015.
- [7] S. Jacobsson, G. Durisi, M. Coldrey, U. Gustavsson, and C. Studer, "Throughput analysis of massive MIMO uplink with low-resolution ADCs," *IEEE Trans. Wireless Commun.*, vol. 16, no. 6, pp. 4038–4051, Jun. 2017.
- [8] C. Risi, D. Persson, and E. G. Larsson, "Massive MIMO with 1-bit ADC," *arXiv pre-print*, 2014. [Online]. Available: <http://arxiv.org/abs/1404.7736>
- [9] T. Hälsig and B. Lankl, "Spatial oversampling in LOS MIMO systems with 1-bit quantization at the receiver," in *Proc. of the Int. ITG Conf. on Systems, Communications, and Coding (SCC)*, Hamburg, Germany, Feb. 2017.
- [10] E. N. Gilbert, "Increased information rate by oversampling," *IEEE Trans. Inf. Theory*, vol. 39, no. 6, pp. 1973–1976, 1993.
- [11] S. Shamai, "Information rates by oversampling the sign of a bandlimited process," *IEEE Trans. Inf. Theory*, vol. 4, no. 4, pp. 1230–1236, 1994.
- [12] T. Koch and A. Lapidoth, "Increased capacity per unit-cost by oversampling," in *Proc. of 26th IEEE Convention of Electrical and Electronics Engineers in Israel (IEEEI)*, Eilat, Israel, Nov. 2010, pp. 684–688.
- [13] L. Landau, M. Dörpinghaus, and G. Fettweis, "Communications employing 1-bit quantization and oversampling at the receiver: Faster-than-Nyquist signaling and sequence design," in *Proc. of the IEEE Int. Conf. on Ubiquitous Wireless Broadband (ICUWB)*, Montreal, Canada, Oct. 2015.
- [14] S. Bender, L. Landau, M. Dörpinghaus, and G. Fettweis, "Communication with 1-bit quantization and oversampling at the receiver: Spectral constrained waveform optimization," in *Proc. of the IEEE Int. Workshop on Signal Processing Advances in Wireless Commun. (SPAWC)*, Edinburgh, U.K., Jul. 2016.
- [15] S. Bender, M. Dörpinghaus, and G. Fettweis, "On the achievable rate of bandlimited continuous-time 1-bit quantized AWGN channels," in *Proc. IEEE Int. Symp. Inform. Theory (ISIT)*, Aachen, Germany, Jun. 2017.
- [16] S. Bender, P. Seiler, B. Klein, M. Dörpinghaus, D. Plettemeier, and G. Fettweis, "Pathways towards Tb/s wireless," in *Proc. of the IEEE Int. Conf. on Ubiquitous Wireless Broadband (ICUWB)*, Salamanca, Spain, Sep. 2017.
- [17] M. T. Ivrlac and J. A. Nossek, "On MIMO channel estimation with single-bit signal-quantization," in *Proc. of the ITG Workshop on Smart Antennas (WSA)*, Vienna, Austria, Feb. 2007.
- [18] A. Mezghani, F. Antreich, and J. A. Nossek, "Multiple parameter estimation with quantized channel output," in *Proc. of the Int. ITG Workshop on Smart Antennas (WSA)*, Bremen, Germany, Feb. 2010, pp. 143–150.
- [19] J. Mo, P. Schniter, N. G. Prelcic, and R. W. Heath, "Channel estimation in millimeter wave MIMO systems with one-bit quantization," in *Proc. of the 48th Asilomar Conference on Signals, Systems and Computers*, Pacific Grove, USA, Nov. 2014, pp. 957–961.
- [20] G. Zeitler, G. Kramer, and A. C. Singer, "Bayesian parameter estimation using single-bit dithered quantization," *IEEE Trans. on Signal Process.*, vol. 60, no. 6, pp. 2713–2726, Jun. 2012.
- [21] G. P. Fettweis, N. ul Hassan, L. Landau, and E. Fischer, "Wireless Interconnect for Board and Chip Level," *Design, Automation & Test in Europe Conference & Exhibition (DATE)*, pp. 958–963, 2013.
- [22] S. Bender, M. Dörpinghaus, and G. Fettweis, "On the achievable rate of bandlimited continuous-time AWGN channels with 1-bit output quantization," *arXiv pre-print*, 2017. [Online]. Available: <https://arxiv.org/abs/1612.08176>
- [23] D. Fertoni, T. Duman, and M. Erden, "Bounds on the capacity of channels with insertions, deletions and substitutions," *IEEE Trans. Commun.*, vol. 59, no. 1, pp. 2–6, Jan. 2011.
- [24] K. Immink, "Runlength-limited sequences," *Proc. of the IEEE*, vol. 78, no. 11, pp. 1745–1759, 1990.